

## Twin Ion Engine Demonstration for Small Spacecraft Applications

Michael Tsay, Riley Terhaar, Kyle Emmi and Carl Barcroft  
Busek Co. Inc.  
11 Tech Circle, Natick, MA 01863, USA; 508-655-5565  
mtsay@busek.com

### ABSTRACT

Two iodine-fueled, second-generation (Gen-2) “BIT-3” gridded RF ion propulsion systems were successfully demonstrated in proximity. The test units feature a host of upgrades from the flight models delivered to Lunar IceCube and LunaH-Map 6U Cube missions onboard NASA’s SLS Artemis 1. Each Gen-2 BIT-3 system is capable of 1.1 mN thrust, 2,150 sec specific impulse and 31.7 kN-sec total impulse, at 75W maximum power input. The twin engines, separated by a mere 6.5 cm, successfully performed simultaneous startup, sequential startup, and throttling, all without noticeable plasma interference. Onboard telemetry confirms that both thruster and cathode pairs operated nominally, and both ion plumes were stable and properly neutralized by the cathodes in all scenarios. This result should give confidence to microsatellite developers who are looking to fulfill propulsion requirements by multiplexing the BIT-3 - a compact, high-TRL, cost-effective, and readily available propulsion module.

### INTRODUCTION

The past decade has seen unprecedented levels of growth in the market for small satellites, particularly in the NanoSat (1-10 kg) and MicroSat classes (10-100 kg). A mere 20 combined NanoSat and MicroSat launches in 2011 has matured into over 400 successful launches in 2021, with expectations that the market will continue to grow exponentially toward 1,000 launches per year by 2025.<sup>1,2</sup> While demand for all classes of micro/nano satellites has risen as a result, the “medium” sized, 20-50 kg MicroSats (including 12U and 27U CubeSats) have seen a marked increase in demand in recent years. Like all small satellites, the cost of MicroSats has decreased due to more affordable system components, decreased launch costs, and the advent of small satellite ride-sharing. At the same time, these satellites support substantial mission-enabling payload volumes (compared to 3-6U CubeSats) and are highly configurable. This ideal balance between low cost and sufficient capability has made the 20-50 kg MicroSats appealing for a wide array of commercial missions in space. When brought together to form a constellation, they can be employed for various LEO applications, such as earth observation, the internet of things (IoT), and high-resolution imaging.<sup>3</sup> Individually, MicroSats can perform deep space scouting missions in preparation for human exploration.<sup>4</sup>

The increasing popularity and broad application of 20-50 kg MicroSats demands low cost, high performance, and sufficiently small propulsion systems. Electric propulsion (EP) has become the primary candidate due to its high specific impulse (Isp) and overall launch

safety, compared to chemical propulsion. However, financial considerations often preclude developing mission-specific EP solutions for medium sized MicroSats. Rather, the market has favored miniature, sub-100W EP devices that were originally developed for 3-6U CubeSats. These engines may be underpowered individually, but they have the benefit of high Technology Readiness Level (TRL) and low Non-Recurring Engineering (NRE) cost. Increasing thrust by clustering is a viable option, though not many thrusters in this class have been tested in a tightly packed configuration.

Among small and mature EP technologies, FEEP/electrospray thrusters have the most flight heritage, especially Enpulsion’s IFM Nano.<sup>5</sup> Accion Systems’ TILE-2 and TILE-3 small-scale electrospray thrusters have also been launched on missions to support 6U class CubeSats in LEO.<sup>6,7</sup> Busek’s first flight model BET-300-P passive electrospray thruster, a derivative of flight-proven technology, has been delivered and is awaiting launch early next year.<sup>8</sup> Electromagnetic EP is also beginning to be employed for small satellite maneuvering, with T4i’s iodine-fueled REGULUS recently demonstrating a maneuver aboard a 12U CubeSat.<sup>9</sup> Even high performance EP (Hall effect and gridded ion), which traditionally requires size and power that are incompatible with small satellites, is now being miniaturized for MicroSats. To this end, ExoTrail has successfully demonstrated the in-flight capabilities of its 50W ExoMG Nano Hall-Effect thruster.<sup>10</sup> In the field of gridded ion technology, ThrustMe’s 1U-sized NPT30-

I2 system recently demonstrated the first iodine EP firing on orbit aboard a 12U CubeSat.<sup>11,12</sup>

For deep-space applications, the University of Tokyo has demonstrated a 30W microwave ion thruster onboard PROCYON, a 50kg-class deep space MicroSat that was launched as a secondary payload on Hayabusa-2 in 2014.<sup>13</sup> Since then, no EP unit has propelled a small satellite into deep space, though that may change in the coming months. Pale Blue's water-based resistojet technology will be the main thruster on EQUULEUS, a 6U deep-space CubeSat mission and secondary payload aboard NASA's upcoming SLS Artemis-1 mission.<sup>14</sup> In a similar vein, Busek's BIT-3, a high-performance gridded ion thruster, will propel two deep-space CubeSats flying on Artemis 1: Lunar IceCube, developed by Morehead State University, will prospect the moon for water-ice deposits, and LunaH-Map, developed by Arizona State University, will map hydrogen enrichments at the lunar South Pole.<sup>15, 16, 17</sup>

### BIT-3 IODINE RF ION PROPULSION SYSTEM

Following the flight unit deliveries to Lunar IceCube and LunaH-Map and a 3,500-hour wear test<sup>18</sup>, Busek updated the BIT-3 RF ion propulsion system design to improve its manufacturability and robustness. The Gen-2 system, shown in Figure 1 and Figure 2, is currently in volume production, with several launches expected in late 2022.<sup>19</sup> Table 1 lists the Gen-2 specifications.

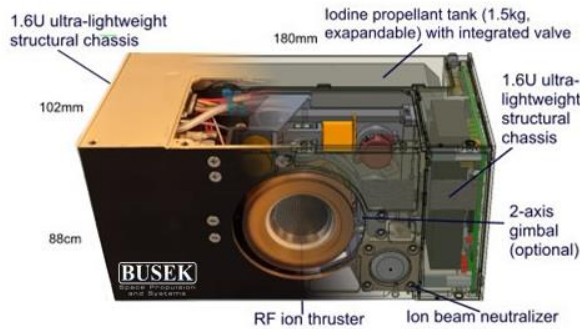


Figure 1: Gen-2 BIT-3 System



Figure 2: Gen-2 BIT-3 Iodine Hot Firing

Table 1: Gen-2 BIT-3 Specifications

BIT-3 Gen 2 Specifications	
System size	180 x 102 x 88 mm (~1.6U)
Thruster type	RF gridded ion engine
Neutralizer type	RF cathode
System mass (wet)	2.9 kg
Propellant load	1.5 kg
System design life	~8,000 hours*
Thrust (nom./min/max)	1.00 / 0.66 / 1.10 mN
Isp (nom./min/max)	1,960 / 1,290 / 2,150 sec
Total impulse	~31.7 kN-sec**
Thrust uncertainty	46 μN
System power (nom./min/max)	70 / 55 / 75W
Operating temperature range	-15 to +45°C
System input format	RS-485, regulated 28V <sub>DC</sub>
Control modes	Register table via RS-485
System TRL	6

\*8,000 hours is tank limited; not fully demonstrated.  
 \*\*Assumes max thrust at 75W PPU input; 12.3 kN-sec demonstrated.

The BIT-3 RF ion thruster utilizes an inductively-coupled plasma (ICP) discharge and a dual-grid configuration, as shown in Figure 3. The inner Screen grid extracts the ions while also serving as the anode. The outer Accelerator grid focuses and accelerates the ion beam, while at the same time preventing back-streaming of neutralizer electrons. Similar to the thruster, the cathode is inherently compatible with reactive propellants such as iodine.<sup>20</sup> Electrons emitted by the cathode neutralize the ion beam via plasma bridge, a purely passive mechanism.<sup>21,22</sup> Operationally, the plasma is started first inside the cathode. The ignition process is instantaneous. Thruster ignition is achieved by momentarily switching the Accelerator grid's polarity to draw in electrons emitted from the cathode. These seed electrons bombard neutral particles in the thruster's discharge chamber, which releases more free electrons and initiates the ICP discharge.

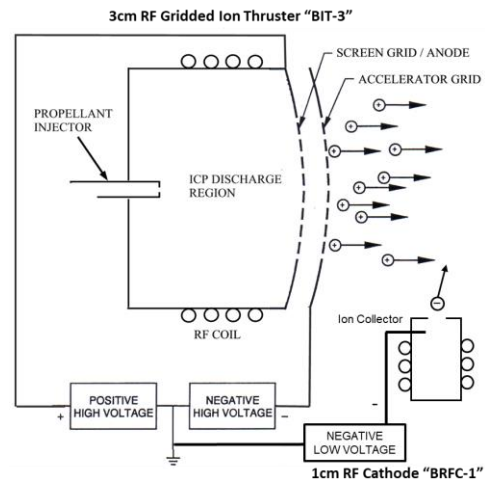


Figure 3: BIT-3 Thruster Configuration

The BIT-3 PPU communicates with the Host via register table read/write over RS-485. Table 2 lists all user-commandable modes in flight. The **Sleep** mode is the system’s default state after power on. The **Warm Standby** mode heats up the entire iodine feed system and places it in a “ready-to-fire” state. The time required to transition from Sleep to Warm Standby depends on the environment and interface temperature. The system needs to be in Warm Standby before it can accept **Thrust** commands.

**Table 2: BIT-3 Flight Modes**

Mode	Brief Description	Nom. Power
<b>Sleep</b>	Minimum power required for communication	3.2W
<b>Warm Standby</b>	Iodine feed system warmed-up and ready to fire	30W during ramp-up; 15-20W to hold
<b>Thrust</b>	Thruster firing at prescribed Thrust Level table	See Thrust Level table

The **Thrust** mode by default puts the system in a 65 W average, 0.89 mN thrust operation. The thrust level can be changed before, during or after a burn to the specifications shown in Table 3. The listed input powers are nominal, time-averaged values, assuming a chassis temperature of 30°C during steady-state operation. If the chassis temperature is cooler, the input power consumption will increase due to the autonomous feed system heater activation, and vice versa. In Thrust mode, the beam current (and therefore the thrust) fluctuates sinusoidally around a target set point at a frequency of 2Hz. This is a result of the thruster’s RF power modulation during close-loop control. Consequently, the input power fluctuates in a similar trend.

**Table 3: BIT-3 Discrete Thrust Levels**

Thrust Level	Avg Input Power, W	I <sub>Beam</sub> , mA	Thrust, mN	Isp, sec
0	42	0	0.01	20
1	55	9.9	0.66	1,290
2	60	11.4	0.78	1,530
3	65	12.9	0.89	1,740
4	70	14.3	1.00	1,960
5	75	15.6	1.10	2,150

It is important to point out that Thrust Level 0 is technically a thrust command but produces almost-zero thrust. It does so by maintaining the cathode and thruster plasma discharge, but reduces the grid voltages to 0, which effectively eliminates ion beam extraction

and hence produces no significant thrust (the 0.01 mN of thrust is produced by the plasma’s thermal velocity). The obvious drawback is the waste of propellant and power (approximately 42 W). The benefit is the ability to transition rapidly to normal thrusting operations without going through the entire ignition sequence. Level 0 is analogous to keeping a car’s engine running at idle.

**TEST OBJECTIVE**

The primary objective of the twin BIT-3 thruster demonstration was to prove that both engines can operate without electrical or plasma interferences during startup and throttling. This project was designed to be a fundamental understanding of the interference mechanisms in twin ion thruster operation. The result would be critical for MicroSat developers looking to employ multiple BIT-3s in proximity. Historically speaking, clustering gridded ion engines is not an issue, as demonstrated by the Japanese Hayabusa mission.<sup>23</sup> This is because gridded ion engines generally are not sensitive to cathode placement, as the cathode is used for neutralizing the ion plume only and not coupled to the thruster’s plasma discharge like in Hall-Effect Thrusters. There are, however, precautions that need to be taken regarding plume field interaction and neutralizer starvation. Plume field interaction can occur if two diverging ion beams are placed too close to each other, where the high-speed ions can collide and scatter slow-moving, charge-exchange ions near the exit plane. This can lead to startup instability issues. Neutralizer starvation, on the other hand, refers to a possible scenario in which a plasma-bridge type cathode is “shared” among multiple thrusters. Since the neutralizer’s electron emission is passive (i.e. the ion beam’s potential draws out a matching number of electrons for neutralization), incorrect cathode placement may lead to excessive electron extraction, causing the cathode discharge to extinguish. A close-proximity, hot fire test was necessary to demonstrate the absence of these phenomena in a practical cluster.

The secondary objective of the test was to validate ion beam neutralization in a twin-engine configuration. Because the vacuum chamber was significantly lengthened for this campaign, the thrusters’ plume was able to “float” electrically, meaning that neutralization had to be performed by the cathodes, rather than the vacuum chamber walls. With two BIT-3s running at the same time, the test was an opportunity to examine the cathodes’ ability to neutralize two ion beams in a relevant environment. The condition for success was obtaining a total cathode current emission greater than or equal to the total ion beam current. Note that over-neutralizing (i.e. cathode current higher than beam current) is not an issue for ground test or on-orbit

operation. On the ground, cathodes sometimes emit more electrons due to facility-interaction (e.g. mobile electrons finding nearby walls). On orbit, CONOPS or the space plasma environment may also force cathodes to emit at a higher level. When cathode emissions are slightly higher than the ion beam current, the charge imbalance will cause the spacecraft bus to float to a small positive potential, which would harmlessly attract excess electrons back to the spacecraft.

## EXPERIMENT SETUP AND FACILITY

Figure 4 and Figure 5 show the twin BIT-3 thruster test setup. Two identical Gen-2 thrusters were placed in parallel, with 6.5 cm chassis-to-chassis spacing. The thrusters were oriented so that the two cathode neutralizers were farthest away from each other. During hot firing, the BIT-3 chassis temperatures were maintained nominally at 30°C via water-cooled fixture plates which simulated a spacecraft mounting interface. Thruster performance was monitored via onboard ion beam current and cathode current telemetries, without an external thrust stand. Two in-situ cameras were used for real-time visual observation.

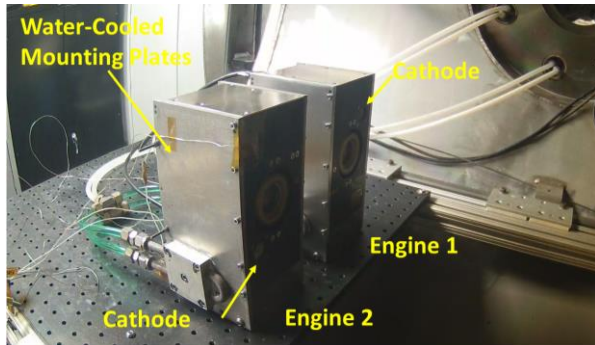


Figure 4: Twin BIT-3 Test Setup, Side View

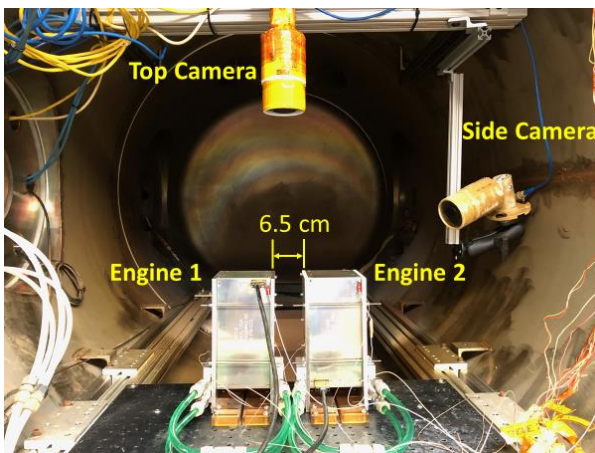


Figure 5: Twin BIT-3 Test Setup, Rear View

The twin engine test was conducted at Busek's T-4 vacuum chamber, shown in Figure 6. The facility was refurbished after a recent, 3,500-hour iodine test and expanded in January 2020 to accommodate the Gen-2 BIT-3 volume production program.<sup>18,19</sup> The upgraded chamber is internally 4 ft in diameter and 8 ft in length, which is large enough to ensure that the BIT-3 plumes were not grounded by the chamber walls. The chambers pumping can maintain a background pressure of  $5 \times 10^{-5}$  torr during twin BIT-3 firings. The two engines were powered by two independent sets of bench DC power supplies. Similarly, RS-485 communications were handled by two sets of desktop computers and LabVIEW user interfaces.



Figure 6: Busek's Upgraded T-4 Vacuum Facility

## RESULTS

Twin BIT-3 thruster firing was successfully demonstrated, as shown in Figure 7. Three operating scenarios were tested, including:

1. Simultaneous startup: both engines started up at the same time from the Warm Standby state, followed by steady burns in Lv5 thrust.
2. Sequential startup: one engine started after another. This scenario simulates unsynchronized startups or single engine flame-out recovery.
3. Throttling: both engines in steady Lv4 burns, followed by unsynchronized throttling down to Lv0, and then back up to Lv4.

Visual observations and telemetry data for each scenario are presented in the following sections. Note that, unless an engine was already running, all startups presented here were initiated from the Warm Standby state, with a Thrust command being sent at Time = 0. During the Warm Standby to Thrust mode transition, the BIT-3 system autonomously executes a series of

deterministic events involving plasma ignition, plasma stabilization, and impedance matching. Nominally, the cathode is ignited ~63 sec after the Thrust command, and the thruster is ignited ~73 sec after a successful cathode turn-on. Thruster ignition is then followed by 35 sec of plasma stabilization and grid voltage increase, at which point a feedback control algorithm takes over and maintains a stable beam current (and thrust) output. The system is then officially in the Thrust state. In total, the process from command to the Thrust state nominally takes 171 sec to complete.



**Figure 7: Twin Gen-2 BIT-3 Iodine Hot Firing**

**Simultaneous Startup**

Due to the 0.5Hz communications rate with the two BIT-3 PPU's and limitations of the laboratory equipment, Thrust command synchronization was difficult to achieve, resulting in a ~0.5sec offset. Despite this, Figure 8 shows that both engines executed ignition sequence near simultaneously and completed the Thrust mode transition at approximately the same time at T = 171 sec (Figure 9).

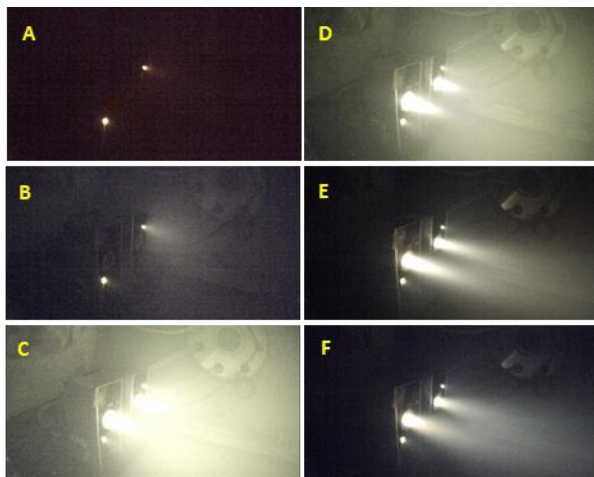


**Figure 8: Twin Engine Simultaneous Startup: A) Cathodes Ignited, B) Cathodes in Boost, C) Thrusters in Grid Polarity Flip, D) Thrusters Ignited, E) Thrusters in Low Grid Voltage, F) Both Thrusters in Nominal Lv 5 Operation**

Both engines fired at Lv4 thrust for ~30 sec, and then throttled up to Lv5 at T = 200 sec. In steady-state operation, the ion beam current responses were nearly identical. The slight discrepancy in the 28V input power (Figure 10) was due to a small variance in chassis temperatures, which resulted in a small difference in the iodine feed system's heater power consumption.

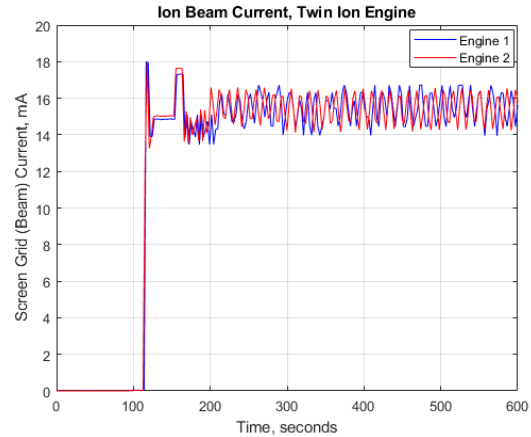


**Figure 9: Beam Current (Simultaneous Startup)**

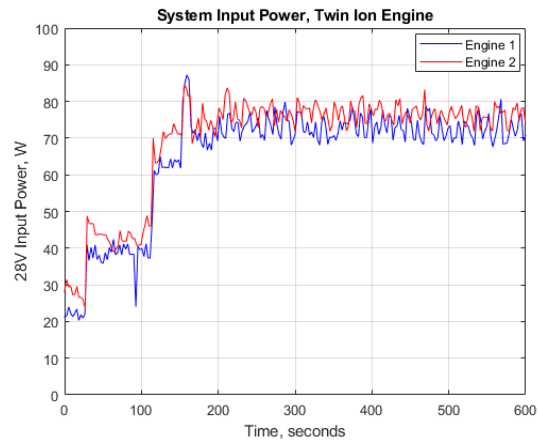


**Figure 10: 28V Input Power (Simultaneous Startup)**

Figure 11 shows the cathode neutralizer's emission current. Both cathodes were lit around the same time at T = 63 sec, followed by idling at 7-8 mA for a period of ~58 sec. At T = 121 sec, the cathodes momentarily switched to the boost mode which increased emission to 44 mA, in preparation for thruster ignition. After the thruster was ignited, as evidenced by the ion beam current formation (Figure 9), the cathode emission mechanism became passive. Without a facility grounding effect, the potential difference between the ion beams and the cathode plasma "pulls" the electrons out of the cathode via a plasma bridge. This results in the cathode emitting an equal amount of current as the

ion beam, but opposite in charge. Interestingly, Figure 11 shows that the Engine 1 cathode seemed to be over-neutralized and Engine 2 under-neutralized, but the combined cathode emission did achieve overall neutralization (Figure 12). This means that the total electron currents and ion beam currents from the two engines are in balance. Further analysis is needed to explain the slight mismatch between the two cathode currents. However, demonstrating the overall neutralization in a twin-engine configuration is a very encouraging result.

In Figure 12, one can notice that there were periods during which the cathodes were emitting electrons without the presence of ion beams. These “active” emissions occur during the early stages of startup (i.e. cathode ignition, idling and boosting). As explained in the Test Objective section, such a charge imbalance due to over-neutralization is not an issue, because excess electrons are easily returned to the spacecraft bus without causing any damage.

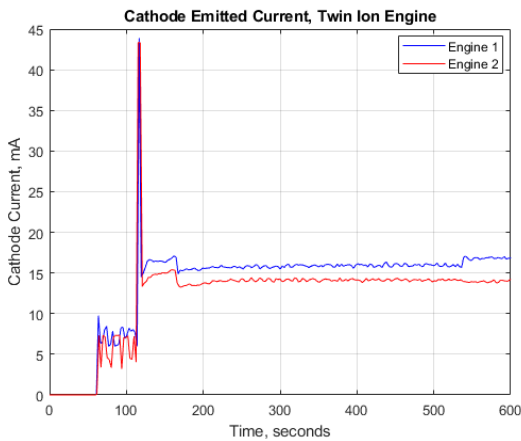


Figure 11: Cathode Current (Simultaneous Startup)

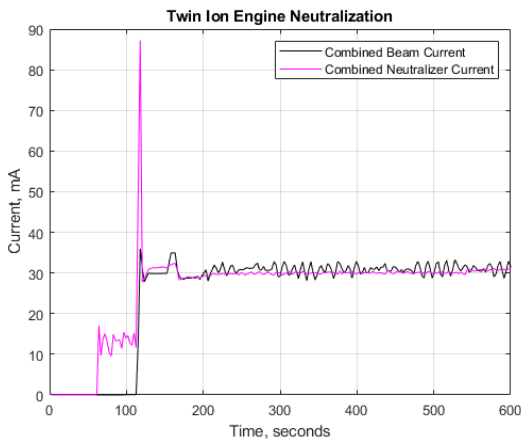


Figure 12: Overall Neutralization (Simultaneous Startup)

### Sequential Startup

The second operating scenario saw Engine 1 already up and running in stable Lv5 thrust, while Engine 2 was commanded to fire at  $T = 0$ . Engine 2 successfully lit and entered Lv4 Thrust mode at  $T = 171$  sec, nominally. Visual (Figure 13) and ion beam current telemetry (Figure 14) both indicated no plasma interference issues. Essentially, the “violent” thruster ignition event in Engine 2 did not cause Engine 1 to flame out or even flicker, suggesting both ion plumes are sufficiently isolated. Figure 15 through Figure 17 show the input power and cathode neutralization results for completeness. The overall neutralization characteristics (Figure 17) are similar to the simultaneous startup case, with the exception that one engine was already running on the background.

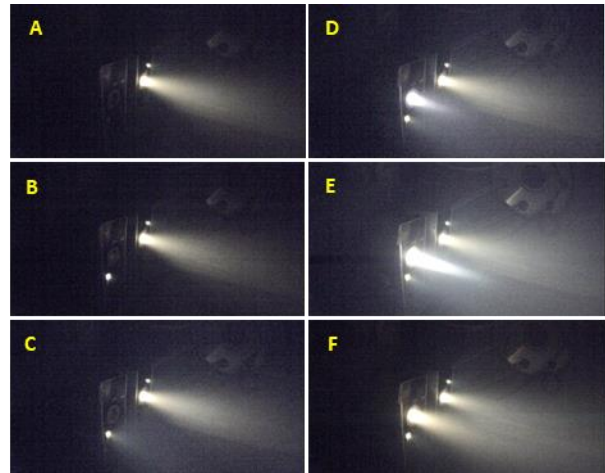


Figure 13: Twin Engine Sequential Startup: A) Engine 1 in Steady Lv5 Thrust, B) Engine 2 Cathode Ignition, C) Engine 2 Cathode in Boost, D) Engine 2 Grid Polarity Flip, E) Engine 2 Thruster Ignition, F) Engine 2 in Steady Lv4 Thrust

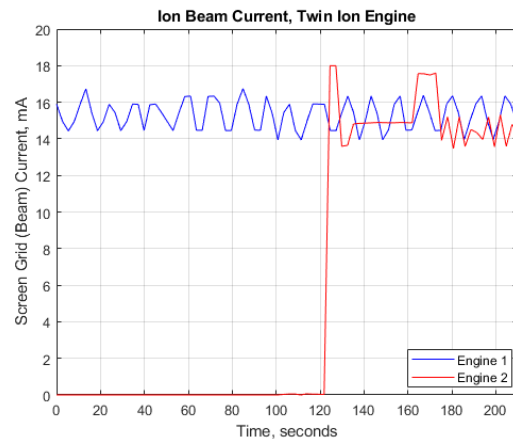
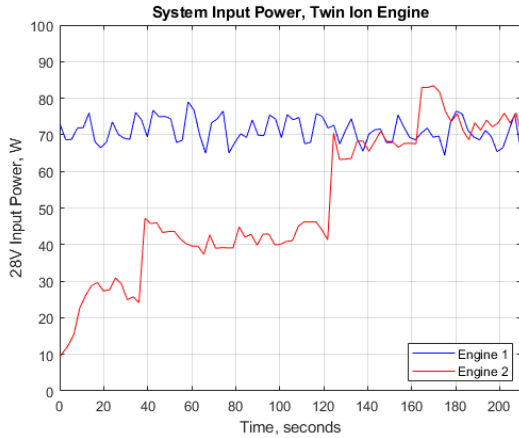
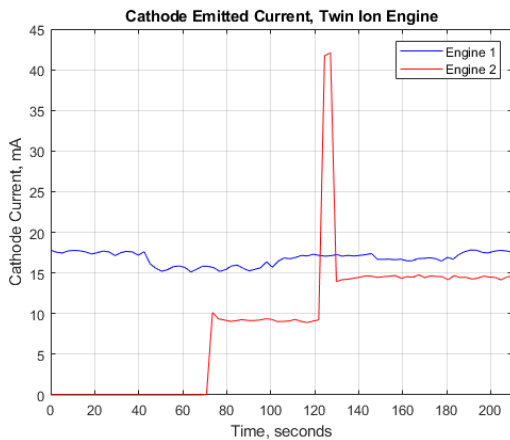


Figure 14: Beam Current (Sequential Startup)



**Figure 15: 28V Input Power (Sequential Startup)**



**Figure 16: Neutralizer Current (Sequential Startup)**

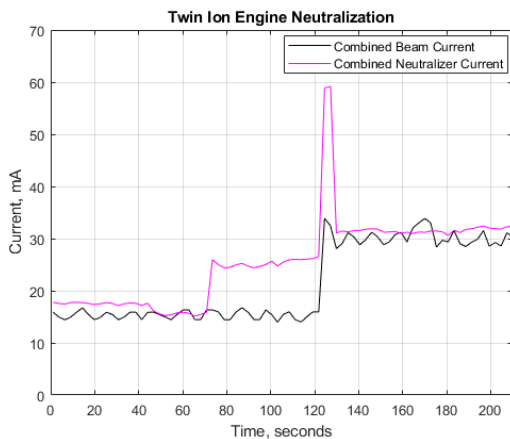


**Figure 17: Overall Neutralization (Sequential Startup)**

**Throttling**

The final scenario tested was throttling, where each engine was independently throttled from Lv4 thrust

down to Lv0 and then back to Lv4. The goal was to test whether the sudden change in grid voltage and beam current in one engine would affect the other engine. The test was successfully carried out, as shown in Figure 18. No abnormal phenomena were observed.

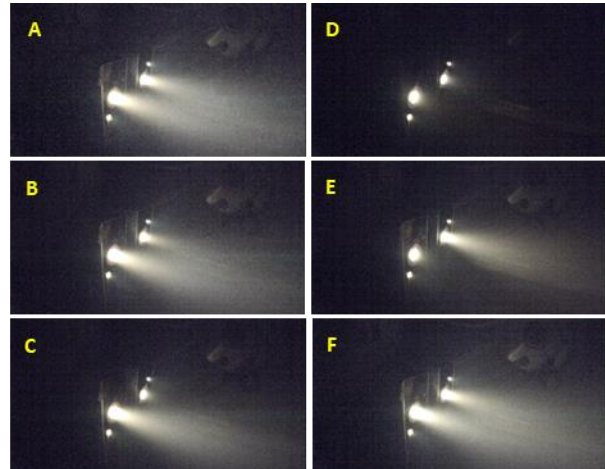


**Figure 18: Twin Engine Throttling: A) Both Engines in Steady Lv4 Thrust, B) Engine 1 Throttling Down, C) Engine 1 in Lv 0 Thrust, D) Engine 2 Throttled Down to Lv 0, E) Engine 1 Throttled Up to Lv 4, F) Engine 2 Throttled Up to Lv 4**

As mentioned previously, Lv0 thrust is a “zero thrust” mode. It does so by keeping the thruster and cathode plasma ON but without applying grid voltages. The result is zero beam current in Lv0, and any small thrust generated is purely due to the plasma’s thermal drift. The beam current data in Figure 19 clearly shows when the engines were throttled down to Lv0 and then back to Lv4. The purpose of Lv0 thrust is demonstrated here: instantaneous thrust generation without going through a 171 sec startup transition. In addition, in Lv0 the power consumption is drastically reduced to ~42W (Figure 20). Of course, the waste of propellant in Lv0 thrust should always be considered when planning on-orbit CONOPS.

The neutralization aspect of the throttling scenario is interesting. When both engines were throttled down at Lv0 (T ~ 82 sec), both cathode emissions reduced to near-idle current, <10 mA, as expected. However, when Engine 1 was down at Lv0 and Engine 2 was at Lv4 (T = 70 sec), Cathode 1 emission did not reduce to idle. Rather, both cathodes showed passive coupling to the lone Engine 2 ion beam, as if they were working as a team. A possible explanation is that due to thermal diffusion, there was still sufficient plasma at the Engine 1 exhaust even when there was no active ion beam. This means that Cathode 1 can still couple to the Engine 2’s plume via a “long” plasma bridge. This phenomenon was repeated for Cathode 2, when Engine

2 was at Lv0 and Engine 1 throttled back up to Lv4 (T = 90 sec). Overall, both cathodes provided more than sufficient neutralizing electron currents for the two ion beams regardless of throttling state, as shown in Figure 22.

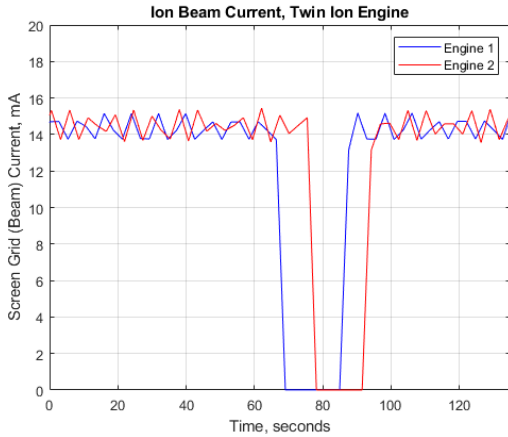


Figure 19: Beam Current (Throttling)

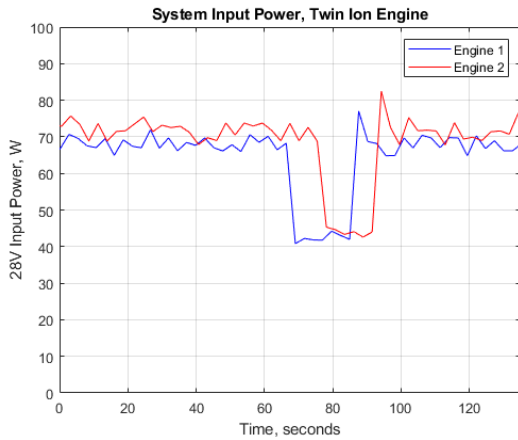


Figure 20: 28V Input Power (Throttling)

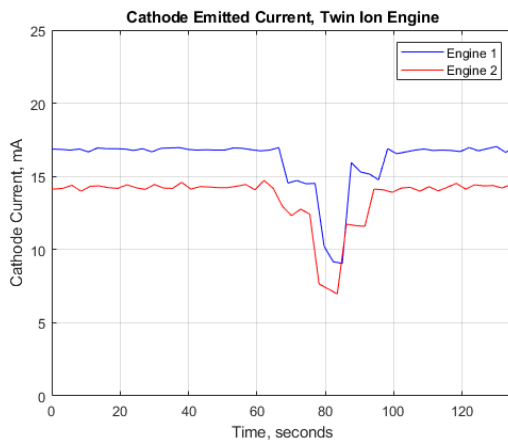


Figure 21: Neutralizer Current (Throttling)

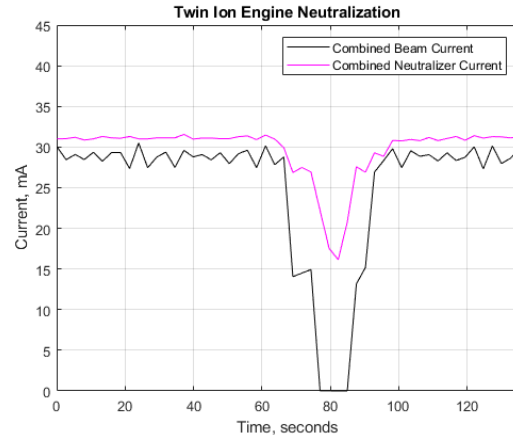


Figure 22: Overall Neutralization (Throttling)

## CONCLUSION

Two Gen-2 BIT-3 propulsion systems were successfully demonstrated side-by-side. The twin engines were separated by 6.5 cm, the closest the mounting fixtures would allow. Three operating scenarios were tested, including 1) simultaneous startup: both engines start up at the same time, 2) sequential startup: one engine starts after another, which simulates unsynchronized startups or single engine flame-out recovery, and 3) throttling: both engines throttled from Lv4 to Lv0 and back to Lv4 unsynchronized. In all scenarios the engines were found to operate nominally without noticeable plasma plume coupling. That is, a drastic change in the plume condition from one engine (startup or throttling) did not cause a flameout or instability on the other engine. In fact, both engines seem to have behaved independently despite their close proximity. In addition to showing operational stability, the ion plumes were found fully neutralized by the cathodes. The two cathodes coupled to the plumes via plasma bridges and were able to emit greater than or equal to the ion beam current in all operating scenarios.

## References

1. Villela, T., et al., "Towards the Thousandth CubeSat: A Statistical Overview," International Journal of Aerospace Engineering, Vol. 2019, pp. 1–13, Jan 2019.
2. Kulu, E., "Nanosatellites Through 2020 and Beyond," 2021 CubeSat Developers Workshop, Apr 2021.
3. Bryce and Space Technology, "SmallSat by the Numbers, 2021," Aug 2021.



- 
4. Cheetham, B., "Cislunar Autonomous Positioning System Technology Operations and Navigation Experiment (CAPSTONE)," ASCEND 2021, Las Vegas, NV, November 2021, AIAA-2021-4128.
  5. Krejci, D., et al., "Development, Production, and Testing of the IFM Nano FEEP Thruster," 36th International Electric Propulsion Conference, Vienna, AUT, September 2019, IEPC-2019-362.
  6. Krejci, D., et al., "Scalable Ionic Liquid Electro Spray Thrusters for Nanosatellites," 39th Annual AAS GNC Conference, Breckenridge, CO, February 2016, AAS16-124.
  7. Schroeder, M., et al., "Maneuver Planning for Demonstration of a Low-Thrust Electric Propulsion System," 34th Small Satellite Conference, August 2020, SSC20-VII-02.
  8. Demmons, N., et al., "Electrospray Attitude Control System Flight Preparation," AIAA SCITECH 2022 Forum, San Diego, CA, January 2022, AIAA-2022-0039.
  9. Bellomo, N., et al., "Enhancement of Microsatellites Mission Capabilities: Integration of REGULUS Electric Propulsion Module into UniSat-7," 70th International Astronautical Congress, Washington, D.C., October 2019, IAC-19-C4-8-B4-5A-5-x52699.
  10. Gurciullo, A., et al., "Experimental Performance and Plume Characterization of a Miniaturized 50W Hall Thruster." 36th International Electric Propulsion Conference, Vienna, AUT, September 2019, IEPC-2019-142.
  11. Martinez, J., et al., "Development and Testing of the NPT30-I2 Iodine Ion Thruster," 36th International Electric Propulsion Conference, Vienna, AUT, September 2019, IEPC-2019-811.
  12. Rafalskyi, D., et al., "In-orbit demonstration of an Iodine Electric Propulsion System," *Nature* Vol. 599, pp. 411–415, Nov 2021.
  13. Koizumi, H., et al., "One-Year Deep Space Flight Results of the World's First Full-Scale 50 Kg Class Deep Space Probe PROCYON and its Future Prospects," 30th Annual Small Satellite Conference, Logan, UT, August 2016, SSC16-III-05.
  14. Asakawa, J., et al., "AQT-D Demonstration of the Water Resistojet Propulsion System by the ISS-Deployed CubeSat," 33rd Annual Small Satellite Conference, Logan, UT, August 2019, SSC19-WKV-07
  15. Malphrus, B.K., et al., "The Lunar IceCube EM-1 Mission: Prospecting the Moon for Water Ice," *IEEE Aerospace and Electronic Systems Magazine*, vol. 34, no. 4, pp. 6-14, 1 April 2019, doi: 10.1109/MAES.2019.2909384.
  16. Clark, P.E., et al., "Preparing for delivery of the Lunar Ice Cube compact IR spectrometer payload," *Proc. SPIE 11505, CubeSats and SmallSats for Remote Sensing IV*, 11505J (22 August 2020); <https://doi.org/10.1117/12.2568027>
  17. Hardgrove et al., "The Lunar Polar Hydrogen Mapper CubeSat Mission," in *IEEE Aerospace and Electronic Systems Magazine*, vol. 35, no. 3, pp. 54-69, 1 March 2020, doi: 10.1109/MAES.2019.2950747.
  18. Tsay, M., "3,500 Wear Test Result of BIT-3 RF Ion Propulsion System," 37th International Electric Propulsion Conference, Cambridge, MA, June 2022, IEPC-2022-255.
  19. Tsay, M., et al., "Volume Production of Gen-2 BIT-3 Ion Propulsion System," 37th International Electric Propulsion Conference, Cambridge, MA, June 2022, IEPC-2022-267.
  20. Tsay, M., et al., "Maturation of Iodine Fueled BIT-3 RF Ion Thruster and RF Neutralizer," 52nd AIAA Joint Propulsion Conference, Salt Lake City, UT, July 2016, AIAA-2016-4544.
  21. Tsay, M., et al., "Neutralization Demo and Thrust Stand Measurement for BIT-3 RF Ion Thruster," 2017 AIAA Propulsion and Energy Forum, Atlanta, GA, July 2017, AIAA-2017-4890.
  22. Scholze, F., et al., "Inductive Coupled Radio Frequency Plasma Bridge Neutralizer," *Review of Scientific Instruments* 79, 02B724, 2008.
  23. Kuninaka, H., et al., "Powered Flight of Hayabusa in Deep Space," 42nd AIAA Joint Propulsion Conference, Sacramento, CA, July 2006, AIAA-2006-4318.